FOAMS

1. Introduction

Foam is a nonequilibrium dispersion of gas bubbles in a relatively smaller volume of liquid. An essential ingredient in a liquid-based foam is surface-active molecules. These reside at the interfaces and are responsible for both the tendency of a liquid to foam and the stability of the resulting dispersion of bubbles. For example, it is common experience that a relatively stable foam can be made by bubbling gas through soapy water, but not through pure water. Important uses for custom-designed foams vary widely from familiar examples of detergents, cosmetics, and foods, to fire extinguishing, oil recovery, and a host of physical and chemical separation techniques. Unwanted generation of foam, on the other hand, is a common problem affecting the efficiency and speed of a vast number of industrial processes involving the mixing or agitation of multicomponent liquids. In all cases, control of foam rheology and stability is desired. These physical properties, in turn, are determined by both the physical chemistry of their liquid–vapor interfaces and by the structure formed from the collection of gas bubbles.

Observed from a distance, foam made from a clear liquid appears homogeneous and white. When observed more closely, however, the intricate structure formed by the close packing of distinct gas bubbles becomes apparent. Figure 1 illustrates several features of this so-called microstructure, which are common to many foams. The sample shown was photographed two hours after thoroughly shaking an aqueous solution of 5% by weight sodium dodecyl sulfate, a common surfactant. Near the top of the sample, most of the liquid has drained away leaving a dry foam consisting of nearly polyhedral gas bubbles separated by thin

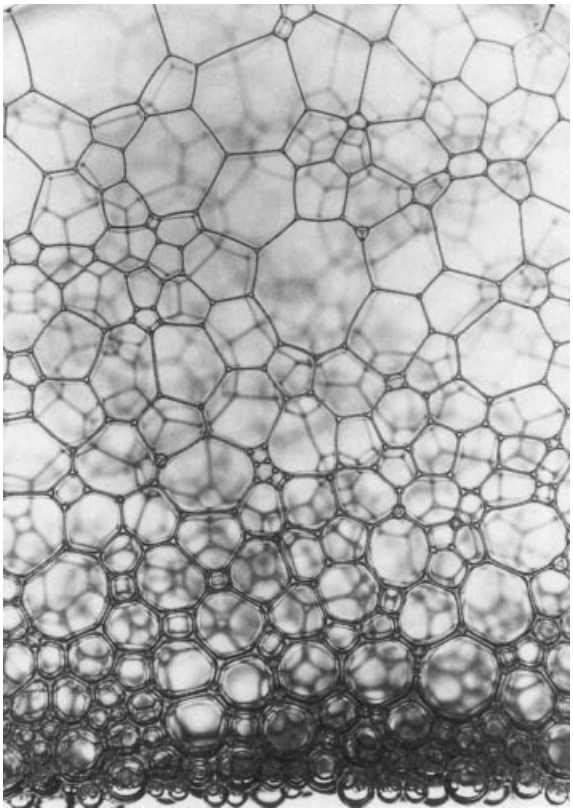

Fig. 1. Photograph illustrating the microstructure of the foam that still persists 2 h after shaking an aqueous solution containing 5% sodium dodecylsulfate. The bubble shapes are more polyhedral near the top, where the foam is dry, and more spherical near the bottom, where the foam is wet. The average bubble size is ~2 mm.

liquid films of uniform thickness. Near the bottom of the sample, by contrast, the foam is relatively wet and consists of bubbles that are more nearly spherical. Whether the bubbles are spherical, polyhedral, or in between, they typically have a distribution of sizes and pack together into a disordered, aperiodic structure. In Figure 1 the average bubble diameter is ~2 mm, but similar structures are also found in foams where the average bubble diameter is varied from 10 μm to 1 cm. In practice, the average bubble size and shape in a foam can be altered for a given liquid according to the production method, the surface-active ingredients, and other chemical additives such as viscosity modifiers or polymeric stabilizers.

The nonequilibrium nature of foams is revealed by the time evolution of their structures. The sample shown in Figure 1 was homogeneous immediately after shaking, but had evolved by the gravitational segregation of liquid downward and bubbles upward prior to being photographed. In addition to drainage, two other mechanisms by which foams evolve are by direct coalescence of neighboring bubbles via film rupture and by the diffusion of gas molecules through

the liquid from small bubble to large bubbles. No matter which of these three processes dominates for a given foam, the liquid and vapor portions invariably consolidate and separate with time; in equilibrium there is no foam, only one region of liquid and one of vapor. The physical chemistry of the interfaces and the foam structure primarily determine the relative rates of the three aging mechanisms.

Foams that are relatively stable on experimentally accessible time scales can be considered a form of matter but defy classification as either solid, liquid, or vapor. They are solid-like in being able to support shear elastically; they are liquid-like in being able to flow and deform into arbitrary shapes; and they are vapor-like in being highly compressible. The rheology of foams is thus both complex and unique, and makes possible a variety of important applications. Many features of foam rheology can be understood in terms of its microscopic structure and its response to macroscopically imposed forces.

2. Physical Chemistry of Interfaces

The chemical composition, physical structure, and key physical properties of a foam, namely, its stability and rheology, are all closely interrelated. Since there is a large interfacial area of contact between liquid and vapor inside a foam, the physical chemistry of liquid–vapor interfaces and their modification by surface-active molecules plays a primary role underlying these interrelationships. Thus the behavior of individual surface-active molecules in solution and near a vapor interface and their influence on interfacial forces is considered here first.

For aqueous solutions, the chemical constituents most commonly responsible for foaming are surfactants, ie, surface-active agents (1). Such molecules find wide use in other settings (see DETERGENCY; SURFACTANTS), and are distinguished by having both hydrophilic and hydrophobic regions. A typical example is the anionic surfactant sodium dodecylsulfate [151-21-3] (SDS). In spite of its hydrophobic hydrocarbon chain, SDS is readily soluble in water due to its polar head group. At concentrations >8 mM (2), the so-called critical micellar concentration (CMC), SDS molecules form spherical micelles where the hydrophobic tails of $\sim$64 molecules clump together so that only their hydrophilic heads are exposed to water (3). At still higher concentrations, even more exotic structures are formed in the bulk solution (1).

2.1. Reduced Surface Tension. Just as surfactants self-organize in the bulk solution as a result of their hydrophilic and hydrophobic segments, they also preferentially adsorb and organize at the solution–vapor interface. In the case of aqueous surfactant solutions, the hydrophobic tails protrude into the vapor and leave only the hydrophilic head groups in contact with the solution. The favorable energetics of the arrangement can be seen by the reduction in the interfacial free energy per unit area, or surface tension, σ. For example, the liquid–vapor surface tension reduces from $\sim$74 to 33 mN/m(= dyn/cm) as the concentration of SDS increases from zero to the CMC (2). Above the CMC, the interface is saturated, the surface tension becomes independent of the bulk concentration, and structures like the micelles start to form in the bulk. In most

custom foams, the surfactant concentration in the base liquid is slightly above the CMC. However, the reduced surface tension is not in itself responsible for the foaming; the primary benefit is that less mechanical energy need be supplied to create the large interfacial area in a foam. The prevention of bubble coalescence needed for significant foaming is accomplished through other physical chemical mechanisms involving surfactants, creating repulsive forces between the bubble surfaces and via the viscoelastic properties of these surfaces.

2.2. Gibbs Elasticity and Marangoni Flows. The reduction of surface tension with increasing surfactant adsorption gives rise to a nonequilibrium effect that can, in some cases, promote foaming. A sudden increase in the interfacial area by mechanical perturbation or thermal fluctuation results in a locally higher surface tension because the number of surfactant molecules per unit area simultaneously decreases. The Gibbs elasticity, E, is often used to quantify the instantaneous change in surface tension σ with area A, ie, $E = d\sigma/d\ln A$. If the film of liquid separating two neighboring bubbles in a foam develops a thickness variations or a surfactant density fluctuation at their interfaces, the resulting local surface tension gradient will induce a Marangoni flow of liquid toward the direction of higher σ. This flow of liquid toward the fluctuations area helps heal the fluctuation and thus keeps the neighboring bubbles from coalescing. Note that the surface rheological parameters are frequency dependent, and that the different processes at the interface scale can have different time scales τ. Then the surface rheological parameters to be considered are those at a frequency $\omega = 1/\tau$. For example, if the time scale for surfactant diffusion and adsorption is shorter than the hydrodynamic time scale, then the Marangoni effect cannot improve stability. Thus the larger the elasticity E, and the longer it takes for surfactant molecules to diffuse to the new surface and reestablish the equilibrium surface excess concentration of surfactant, the more stability is promoted by the Marangoni flows. In practice, the Marangoni effect can cause severe foaming problems in industrial processes, but it alone never suffices to give a stable foam. Too high values of E are nevertheless unfavourable regarding film rupture, and one usually consider that finite values of E, of a few tens of mN/m, are the most suited for good foamability and foam stability.

2.3. Interfacial Forces. Neighboring bubble surfaces in a foam interact through a variety of forces that depend on the composition and thickness of liquid between them, and on the physical chemistry of their liquid–vapor interfaces. For a foam to be relatively stable, the net interaction must be sufficiently repulsive at short distances to maintain a significant layer of liquid in between neighboring bubbles. Otherwise two bubbles could approach so closely as to expel all the liquid and fuse into one larger bubble. Repulsive interactions typically become important only for bubble separations smaller than a few hundredths of a micrometer, a length small in comparison with typical bubble sizes. Thus attention can be restricted to the vapor–liquid–vapor film structure formed between neighboring bubbles, and this structure can be considered essentially flat.

2.4. van der Waals Interaction. The van der Waals force, also known as the London or dispersion force, always attracts adjacent bubbles together and is therefore destabilizing to foams. This attraction is ultimately of quantum mechanical origin, where like molecules are attracted through the electric fields

associated with fluctuations in their instantaneous dipole moments. Summing up these molecular forces over all molecules in a flat film of thickness $\hbar$ and infinite extent, the interaction energy per unit area is $V_{\mathrm{VDW}}(\hbar) = -A/12\pi\,\hbar^2$ where A is the Hamaker constant. For a film of water in air, $A = 3.7 \times 10^{-21}$J (4); for other liquids its value is still close to the thermal energy k_BT, which sets the scale for van der Waals interactions.

Electrostatic Double Layer Interaction. To prevent the film from thinning to zero thickness under influence of the van der Waals interaction, a balancing repulsive force is required. One possibility is the electrostatic double-layer interaction resulting from the mutual repulsion of charge clouds residing at each side of the film due to the dissociation of surface-adsorbed ionic surfactants. The thickness of the diffuse double layer of charges is roughly the debye screening length $1/\kappa_D$, whose value is determined by electrolyte content. For 1:1 electrolytes such as NaCl, $1/\kappa_{\mathrm{D}} \approx 1/\sqrt{}10.8\rho$ nm, where ρ is the molar bulk electrolyte concentration. The electrostatic double-layer interaction energy per unit area is given by $V_{\mathrm{DL}}(\hbar) \approx (64k_{\mathrm{B}}T\rho\ \gamma^2/\kappa_{\mathrm{D}})\ \exp(-\kappa_{\mathrm{D}}\hbar)$, where γ is a factor of order unity for highly dissociated ionic surfactants (4). In practice, the interaction strength may be estimated from knowledge of the liquid solution's pH and electrical conductivity.

The combined effect of van der Waals and electrostatic forces acting together was considered by Derjaguin and Landau (5) and independently by Vervey and Overbeek (6), and is therefore called DLVO theory. It predicts that the total interaction energy per unit area, also known as the effective interface potential, is given by $V(\hbar) = V_{\mathrm{VDW}}(\hbar) + V_{\mathrm{DL}}(\hbar)$. In the absence of externally imposed forces, the equilibrium thickness of the liquid film separating two bubbles is found by minimizing $V(\hbar)$ with respect to $\hbar$. This is demonstrated in Figure 2 for an aqueous film containing 1 mM of 1:1 electrolyte. For this case, the minimum is located near 130 nm, but is too shallow to be seen in comparison with the energy barrier which keeps the film thickness away from the deep van der Waals minimum at zero thickness. In that range of thickness (from a few tens of nm to a few hundred) the thin film are usually called $\ll$ common black films.

Other Interactions. In practical situations, quantitative application of DLVO theory may be uncertain due to uncontrolled Hamaker constants, screening lengths, or dissociation constants.

When the electrostatic energy barrier is overcome, the films can still be stabilized at extremely low thickness ($<$0.5 nm) via entropic confinement forces (steric forces). Such extremey thin films are then called Newton Black films. The solvation forces are then typically due to molecular structure in the liquid that plays a role when the film is thinner than several molecular diameters, and can be either attractive or repulsive. An example is the repulsive hydration force due to water hydrogen bonding with the polar head group of a surfactant molecule adsorbed to the liquid–vapor interface (7,8).

Other steric repulsions can arise and stabilize the film at higher thickness in the case where the interfaces are covered by thick polymeric layers (either flattened on the surface or in a brush-like structure).

Beside these first forces in thin films, others come from the supramolecular structuringof the surfactant within the thin films (8,9). These structural forces can be extremely long range and are oscillatory, having a periodicity set by the effective size of the structures responsible for the forces. A supramolecular

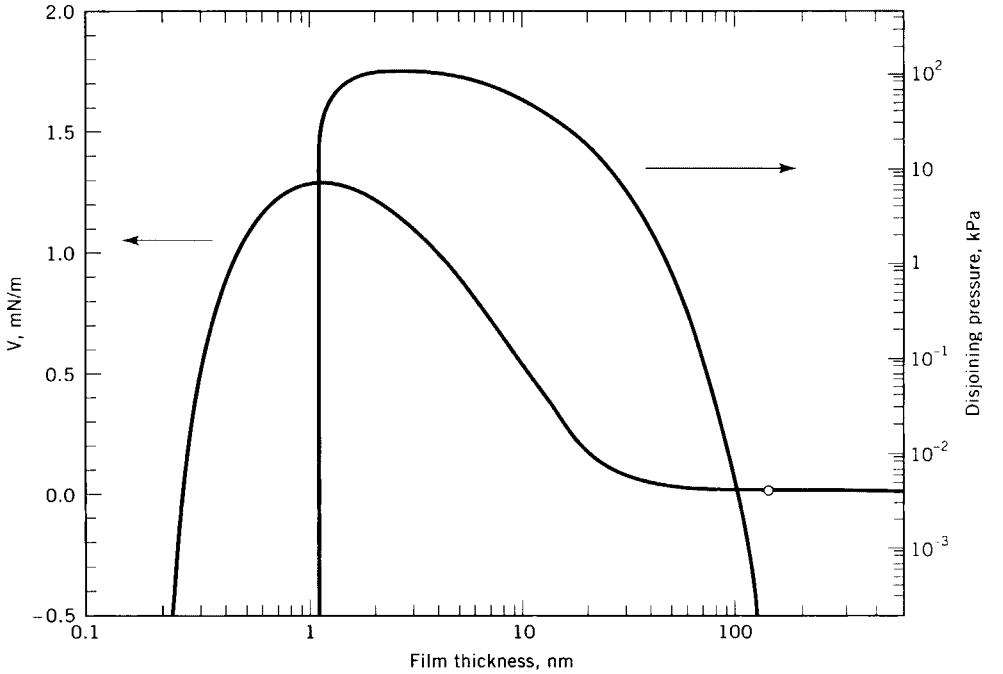

Fig. 2. Effective interface potential (left) and corresponding disjoining pressure (right) vs film thickness as predicted by DLVO theory for an aqueous soap film containing 1 m M of 1:1 electrolyte. The local minimum in $V(\hbar)$, marked by °, gives the equilibrium film thickness in the absence of applied pressure as 130 nm; the disjoining pressure $\Pi = -dV/d\mathrm{l}$ vanishes at this minimum. The minimum is extremely shallow compared with the stabilizing energy barrier. To convert kPa to atm, divide by 10^2. mN/m = dyn/cm = ergs /cm^2.

ordering means that the forces can only be found for high surfactant concentrations (well above the CMC). The structure most usally found in thin films are layers of surfactant micelles or stacked bilayers. Thin films containing both surfactant at the interfaces and polylectrolytes (charged polymers) in bulk also show supramolecular organization in thin films. In general, the more components the system contains, the more degrees of freedom exist for structure within the film which cannot be accounted for by DLVO.

Disjoining Pressure. A static pressure difference can be imposed between the interior and exterior of a soap film by several means including, eg, gravity. In such cases the equilibrium film thickness depends on the imposed pressure difference as well as on the effective interface potential. When the film thickness does not minimize $V(\hbar)$, there arises a disjoining pressure $\Pi = -dV/d\ \hbar$ which drives the system toward mechanical equilibrium. In response to a hydrostatic pressure, the film thickness thus adjusts itself so that the disjoining pressure balances the applied pressure and mechanical equilibrium is restored.

The disjoining pressure versus film thickness as predicted by DLVO theory for an aqueous film containing 1 mM of 1:1 electrolyte is shown along with the effective interface potential in Figure 2. The equilibrium thickness of a free film is where the effective interface potential is at a local minimum or, equivalently,

where the disjoining pressure vanishes with a negative slope. If the same film is not free, but instead rises vertically from solution in the presence of the earth's gravitational field, its thickness will vary in response to the height dependence of the hydrostatic pressure. For example, at ~8 cm above the solution the hydrostatic pressure in the film drops by ~10 kPa and, according to Figure 2, the film thickness at this height must decrease to 30 nm in order to be in equilibrium. Similar considerations are important for establishing the distribution of liquid around several bubbles packed together in a foam, and hence the bubble shapes. The thin-film balance apparatus allows to create and study a single thin film, held on a horizontal support, and at any applied pressure. Hence, this method provides measurement of disjoigning pressures vs film thickness (8,9).

Although the details of the interaction between neighboring bubble surfaces in a thin flat film may not be accurately described by the simplest DLVO theory, it nevertheless captures the essential physics. There is a large energy barrier, which prevents two films approaching too closely. This energy barrier may arise from electrostatic repulsion, as in the DLVO model, or it may arise from other interactions. However, its role is primarily to prevent two films from approaching sufficiently close that they fall into the deep attractive well. The degree to which the two films are forced together by external forces determines how high up the energy barrier they are forced; this is in turn parameterized by the disjoining pressure. Should the repulsive barrier be overcome, the films fall into the attractive minimum, whereupon they coalesce. Thus this repulsive barrier provides the essential stabilization of the foam.

Based on the underlying physical chemistry of surfactants at interfaces, important features of foam structure, stability, rheology, and their interrelationships can be considered as ultimately originating in the molecular composition of the base liquid.

2.5. Structure. *Very Wet Foam: Froth.* Foam structure is characterized by the "wetness" of the system. Foams with arbitrarily large liquid to gas ratios can be generated by excessive agitation or by intentionally bubbling gas through a fluid. If the liquid content is sufficiently great, the foam consists of well-separated spherical bubbles that rapidly rise upwards displacing the heavier liquid. Such a system is usually called a froth, or bubbly liquid, rather than a foam. When the bubbles in a froth reach the surface, they may instantly burst, they may seethe and gradually burst, or they may collect together and form a more proper foam, all according to the quantity and nature of the surface active components in the liquid. This is familiar to anyone who has noticed the difference in opening agitated bottles of seltzer water and beer. There are no surface-active components in the former, and hence there are no interfacial forces or Marangoni effects to hinder the direct coalescence of bubbles.

Wet Foam: Spherical Bubbles. If there are sufficiently strong repulsive interactions, such as from the electric double-layer force, then the gas bubbles at the top of a froth collect together without bursting. Furthermore, their interfaces approach as closely as these repulsive forces allow; typically on the order of 100 nm. Thus bubbles on top of a froth can pack together very closely and still allow most of the liquid to escape downward under the influence of gravity while maintaining their spherical shape. Given sufficient liquid, such a foam can resemble the random close-packed structure formed by hard spheres. With less

liquid, depending on the distribution of bubble sizes, the bubbles must distort from their spherical shapes. For example, spheres of identical size can pack to fill at most $\pi/\sqrt{18} \approx 0.74$ of space; this occurs if they are packed into a crystalline lattice. A foam with a monodisperse size distribution but $<26\%$ liquid is thus composed of bubbles which are not spherical but are noticeably squashed together. Typical foams, as in Figure 1, have a fairly broad distribution of bubble sizes and can therefore maintain spherical bubbles with significantly less liquid. Empirically, foams with greater than $\sim 5\%$ liquid tend to have bubbles that are still approximately spherical, and are referred to as wet foams. Such is the case for the bubbles toward the bottom of the foam shown in Figure 1. Nevertheless, it is important to note that even in the case of these wet foams, the bubbles are deformed, if only by a small amount.

Dry Foam: Polyhedral Bubbles. A dry foam, by contrast, is one with so little liquid that the bubbles are severely distorted into approximately polyhedral shapes. Typically this occurs for foams with $<1\%$ liquid by volume, as is the case for the bubbles toward the top of the foam shown in Figure 1. The structure of polyhedral foams is more appropriately described in terms of the liquid films separating neighboring bubbles rather than in terms of the packing of bubbles as individual units. Most of the interfacial area in a polyhedral foam is in the form of polygonal liquid films having uniform thickness and separating two adjacent gas bubbles. The structure formed by these films is seemingly random, but nevertheless possesses a certain regularity which follows from mechanical constraints. The first of these is that only three films can mutually intersect, and they must meet at an angle of 120°. The intersection of four films is unstable and breaks up into two sets of three because the surface tension of the films exerts a force which acts to minimize the total interfacial area. The region of intersection formed by three films is known as the Plateau border in honor of the Belgian physicist J.A.F. Plateau, who first studied their properties. It is the Plateau borders, rather than the thin liquid films, which are apparent in the polyhedral foam shown toward the top of Figure 1. Lines formed by the Plateau borders of intersecting films themselves intersect at a vertex; here mechanical constraints imply that the only stable vertex is the one made from four borders. The angle between intersecting borders is the tetrahedral angle, $\cos -1(-1/3) \approx 109.47^\circ$. In terms of the arrangements of gas bubbles, the rules describing the structure of a polyhedral foam may be summarized as follows. First, only sets of four bubbles may be in mutual contact. All four bubbles share a common vertex, each of the four combinations of three bubbles share a common Plateau border, each of the six combinations of two bubbles share a common film, and the angles between pairs of films and between pairs of borders are, respectively, 120° and the tetrahedral angle.

These local structural rules make it impossible to construct a regular, periodic, polyhedral foam from a single polyhedron. No known polyhedral shape that can be packed to fill space simultaneously satisfies the intersection rules required of both the films and the borders. There is thus no ideal structure that can serve as a convenient mathematical idealization of polyhedral foam structure. Lord Kelvin considered this problem, and his tetrakaidecahedron is still considered the best periodic structure of identical polyhedra that can nearly satisfy the mechanical constraints, while providing the smallest surface energy (or area).

A more efficient structure for minimizing the surface energy, has more recently been proposed (known as the Weaire-Phelan structure (10), but it consists of bubbles of two different types, and whether it is the optimal structure remains an open question.

A real foam has further degrees of freedom available for establishing local mechanical equilibrium: the films and Plateau borders may curve. In fact, curvature can be readily seen in the borders of Figure 1. In order to maintain such curvature, there must be a pressure difference between adjacent bubbles given by Laplace's law according to the surface free energy of the film and the principle radii of curvature of the film: $\Delta P = \gamma_f \cdot (r^{-1}_1 + r^{-1}_2)$. Note that the pressure inside a bubble must be constant. The Laplace pressure is determined by the regions of greatest curvature. Thus, at the facets of the bubble where the surface is nearly flattened and the curvature is decreased, force balance is maintained by the effects of the disjoining pressure, which must balance the Laplace pressure in the regions of high curvature.

Even though pressure differences can exist between adjacent bubbles, and between the gas and the liquid, the pressure throughout the continuous liquid structure of films, borders, and vertices must be constant; otherwise, liquid flows until all pressure gradients vanish. Figure 3(**a**) shows a cross-section of three films meeting in a Plateau border, and illustrates how pressure balance is achieved between liquid residing in a film and liquid residing in a border. Since the films are flat and opposite faces are parallel away from the border, the pressure inside the film equals the pressure in the gas minus the disjoining pressure $\Pi(\hbar)$. In the border, by contrast, the pressure equals the gas pressure minus the Laplace pressure σ/r, where r is the radius of curvature of liquid–vapor interface at the Plateau border. The pressure balance is thus achieved

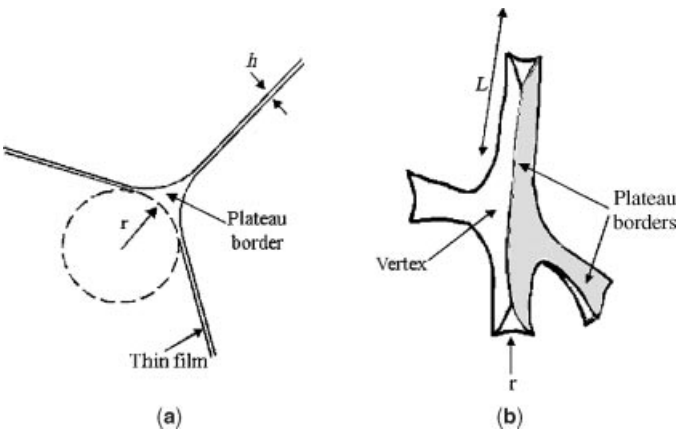

Fig. 3. (**a**) Two-dimensional schematic illustrating the distribution of liquid between the Plateau borders (radius r) and the films (thickness h) separating three adjacent gas bubbles (spehere equivalent radius R). For dry foams, $h \ll r \ll R$ (R, the bubble radius). (**b**) Three-dimensional (3D) schematic of the basic liquid structure in a foam : four Plateau borders connected at a vertex. For wet foams, the Plateau border length L is not much bigger than r, and the liquid inside the vertex can no longer be neglected.

by adjusting the distribution of liquid between films and borders until the disjoining pressure equals the Laplace pressure $\Pi(\hbar) = \sigma/r$.

The liquid distribution inside the different structures of the foam (Plateau borders, vertex and thin films), and their relative weights depend on the overall liquid fraction ϵ. In the limit of dry foams, and up to a few percent of liquid fraction, one can consider that all the liquid is contained inside the single Plateau borders. In that case, the bubbles are tightly packed, and the plateau border radius are much smaller than the bubble size D (or the Plateau borders length). One can then write that $r \approx D\epsilon^{1/2}$. So the dryer the foam, the smaller the radius of the PB, and the higher the capillary and disjoigning pressures. For wet foams, in one hand, the Plateau borders are strongly swollen, so that their radius r is no longer much smaller than their length L (Fig. 3). On the other hand, the volume of the vertex is on the order of r^3, and thus can no longer be neglected, as compared to the one inside a border (on the order of r^2L). The volume of liquid inside the thin films is always negligible when compared to the one inside the Plateau borders and the vertex. Indeed, thin film thickness are in the range of a few tens of nm, while r is a few hundred of microns for millemeter size bubbles: so, $h \ll r < D$, and this remains valid in the more ordinary situations of bubble sizes and liquid fractions.

Measurement. A complete characterization of the structure of a foam requires a characterization of the structure of the bubbles that comprise the foam. The total liquid content can be readily found from the mass densities of the foam and the liquid from which it was made. However, a more detailed determination of the bubble structure, including their average size, their shape, their structure and their size distribution is much more difficult, and is typically impeded by the problems in visualizing the interior of a foam. Even in the absence of any intrinsic optical absorption of the liquid, the strong mismatch in the indexes of refraction between the gas and the fluid results in a large scattering of light, usually precluding direct visualization of the interior structure of a foam. As a result, other, less direct, methods have been developed, and must be used, except in exceptional cases where the foam structure has been optimized for visualization.

To date, the most detailed characterization of the full 3D structure of a foam is that by E. B. Matzke in 1946 (11). The method was to place by hand 1900 identical bubbles one at a time into a dish roughly 14 bubbles in diameter and then to image the structure with a dissecting microscope. After repeating this procedure 16 times, the most abundant bubble shape was found to be a 13-sided polyhedron having 1 quadrilateral, 10 pentagonal, and 2 hexagonal faces. The number of faces per bubble ranges from 11 to 18, and is 13.7 on average. This can be compared with the theoretical result 13.39 for a statistical foam with isotropic cells of equal volume based on the structural rules given earlier and Euler's theorem (12,13). Such theory has recently been generalized to foams with curved faces (14).

Although informative, the technique of Matzke is restricted to use on the small class of very dry foams that have large cells and are essentially transparent to visible light. No such painstaking measurement and analysis have been carried out on foams with a more naturally broad bubble size distribution, like the one shown in Figure 1. However, one optical imaging technique that

circumvents the problem of multiple light scattering and thus can be used more generally is to estimate the bubble size distribution from the area individual foam bubbles occupy at a glass surface. Such experiments, and the systematic differences between bulk and surface bubble distributions, have been reviewed (15). Another technique that also directly measures the bubble size distribution is the use of a Coulter counter, where individual bubbles are drawn through a small tube and counted (16). This yields a direct measure of the bubble size distribution, but it is invasive and cannot probe the structure of the foam. One technique that does probe the foam structure directly is cryomicroscopy. The foam is rapidly frozen, and the solid structure is cut open and imaged with an optical or electron microscope (17). Such methods are widely applicable and provide a direct image of the foam structure; however, they destroy the sample and may also perturb the foam structure in an uncontrolled manner during the freezing. Noninvasive measurements done by optical tomography (18), on a typically 10–20 bubble dry foam, provided results very close to the one of Matzke. The X-ray tomography technique is under development and should give intensive results in the next years.

Beside experimental techniques, a lot of information on foam structure can be obtained by numerical simulations. Such simulations have strongly benefit of the development of the free software "Surface Evolver" by Brakke (19). Using this software, Kraynik and co-workers. have found again a good agreement with the Matzke's data, evidencing for instance the great number of pentagonal faces in equilibrated foams, and an average number of faces per cell $\sim$13.7 (20). The study of the role of polydispersity on the foam structure and bubble types is also an ongoing work.

Other methods attempt to probe the structure of the foam indirectly, without directly imaging it. For example, since the liquid portion of the foam typically contains electrolytes, it conducts electrical current, and much work has been done on relating the electrical conductivity of a foam to its liquid content, both experimentally (21) and theoretically (22,23). The value of the conductivity depends in a very complex fashion on not only the liquid content and its distribution between borders and nodes, but the geometrical structure of the bubble packing arrangement. Thus electrical precise quantitative measurements of the gas:liquid ratio are still difficult as it needs some calibration; however this technique is useful for determining spatial and temporal variations of the liquid fraction (using arrays of electrode pairs disposed at different location in a foam). In any case, the mean liquid fraction of a foam can still be accurately estimated from the foam's mass density.

Another nonimaging technique has been developed that exploits the strong multiple light scattering in foams, and provides a direct, noninvasive probe of bulk foam structure and dynamics (24–26). The time-averaged transmission of light through a foam gives a measure of the average bubble size, while temporal fluctuations in the scattered light intensity probe the motion of bubbles within the foam.

2.6. Stability. Control of foam stability is important in all applications, whether degradation of a custom foam is to be minimized or whether excessive foaming is to be prevented. In all cases, the time evolution of the foam structure provides a natural means of quantifying foam stability. There are three basic

mechanisms whereby the structure may change: by the gravitational segregation of liquid and bubbles, by the coalescence of neighboring bubbles via film rupture, and by the diffusion of gas across the liquid between neighboring bubbles.

2.7. Drainage. All foams and froths consist of liquid and vapor components that have very different mass densities, making them susceptible to gravitationally induced segregation. In very wet froths the vapor bubbles rapidly move upward while the liquid falls. In longer lived foams, the gas fraction is higher and the bubbles are tightly packed. Nevertheless, the heavier fluid may still drain downward through the foam liquid network between the bubbles. As time proceed, some liquid drains out and accumulates at the bottom of the foam, while the overall liquid fraction of the foam decreases. Provided there is no rupture of the films, this free drainage proceeds until there develops a vertical, hydrostatic pressure gradient to offset gravity. This results in a nonuniform gas:liquid volume fraction with the foam being more wet near the bottom of the container as in Figure 1.

Experimentally, as an alternative to the free drainage situation, the forced drainage experimental procedure is often used for determining the typical drainage speeds and rates within a foam. In a forced drainage experiment, the surfactant solution is injected, at a controlled flow rate, at the top of an intially drained foam. A well-defined and stable wet front develops in the foam, and propagates at a constant velocity, and which dependence with the foam parameters (bubble size, nature of the surfactant, liquid viscosity, for instance) can be obtained. For both free drainage and forced drainage, the spatial and temporal variations of the liquid fraction, providing the liquid profile inside the foam at any time, have been successfully measured by electrical conductivity (27), light scattering techniques (either in the limit of multiple scattering with no additives (28,29), or with fluorescent probes added (30)). As the liquid in a foam is principally distributed inside the network of Plateau Borders, connected at the vertex, drainage corresponds to the flow of liquid inside this skeleton of interconnected tubes. Foam drainage can thus be related to liquid flows inside porous media. Note here that the particularity of foams is that the Plateau border cross sections (the pore size) is dinamycally coupled to the liquid content: Plateau borders and vertex are deformable, and can shrink or swell depending on the amount of liquid inside them.

Based on the assumptions that the liquid flows only inside the Plateau Border network, and that the liquid fractions remain low, drainage equations, describing the spatio-temporal evolution of the liquid fraction, have been derived, corresponding to different drainage regimes and microscopic properties of the flow inside the structure (27,30–32). Drainage speeds straightforwardly increase with the bubble size, the foam liquid fraction,and decrease with the bulk liquid viscosity, but they also depend in a complex manner on the nature of the surfactant used, via their effect on the interfacial properties of the bubbles. The bulk flow inside the Plateau borders is in fact coupled to the flow within their surfaces. A dimensionless parameter M, $M = \mu r/\mu_s$ (r is the Plateau border radius, μ_s the surface shear viscosity and μ the bulk viscosity) was first introduced by Leonard and Lemich (33), to describe the mobility of the surface and the bulk/surface coupling. For low values of M, the surface can be considered as immobile and rigid, providing a Poiseuille flow inside the Plateau borders: In this first

regime of drainage, the drainage velocity is then proportional to the liquid fraction. In the limit of high M, a second drainage regime is found: The surfaces are mobile and flow partially with the bulk solution. Thus the hydrodynamic resistance of the Plateau Borders is small, as the flow is approaching a plug-like type. The main dissipation is then located inside the vertex.This change of dissipation localization changes the drainage properties, and, eg, the dependence of the liquid velocity with the liquid fraction, which becomes proportional to its square root. The drainage data, obtained under a very large range of experimental conditions (corresponding to more than three order of magnitude of the parameter M) finally fit very well within this simple two regimes description, with a cross-over between the two regimes for M spanning between 0.8 and 3 (34). Experiments at the scale of a single Plateau Border inside a foam, done by confocal microscopy, are in agreement with the drainage results on macroscopic foams, and have confirmed the role of the surface mobility on the type of flow (35).

The agreement between the drainage and the models based only the flow inside the Plateau borders and the vertex show that the thin films do not participate directly in the liquid transport, and can be neglected when one considers the drainage of a macroscopic foam. This has also been found in numerical simulations (36), and it is consistent with the fact that the liquid contained inside the films is always much smaller than the one inside the Plateau Border network. However, there are some coupling between the downard flow inside the PB and circulation motions often seen inside the films. The result of this interaction is to set the velocity boundary conditions at the three corners of the Plateau borders (where they are connected to the films). These boundary conditions are in fact important regarding the shear inside the surface (33,34,36).

At their own scale, the thin films also drain inside the surrounding Plateau borders, as the liquid is sucked by the lower pressure inside these borders. Thickness variations in a draining soap film can be observed by eye via the colors reflected under white light illumination. A large number of experiments has also been done on soap films pulled at constant speed from a soapy liquid (37–39). In addition to simple laminar flows set by film thickness, liquid viscosity, and here again the surface mobility, whole regions of thick film can flow like a plug into the Plateau border and exchange for regions of thin film, probably nucleated close to the Plateau border and in relation with local pinching effects. This process is called marginal regeneration (37) and is believed to be important in foams as a means of bringing liquid from the films into the Plateau borders. When supramolecular structures get confined inside the thin films as they drain, the oscillatory nature of the resulting supramolecular forces induce a stepwise thinning. The film drains in discrete thickness steps, and confined layers are consecutively pealed off the film. This stratification effect inside the film allow an indirect measurement of effective micelle or surfactant bilayer sizes. For polymer/surfactant mixtures, it is found that the thinning step size corresponds to the polymer network meshsize (9).

Drainage rates and speed also depend on the gas used. This is due to a coupling between the coarsening process (see below) and the drainage flows. The coupling is efficient when the typical times scales of both processes are close, and in that case, this results in an acceleration of the drainage rates (40,41). Finally, drainage depends also on the size and shape of the container as well (28–42).

On the ground, getting rid of drainage is not an easy task, and no efficient solutions has ever been found. In the forced drainage setup, a continuous injection of liquid at the top, at the same flow rate as the foam drain, is difficult to achieve, and convective instabilities occurs as soon as the flow rate (43,44). Sample rotation apparatus, where the direction of gravity is alternatively changed, can work but only for limited conditions of bubble sizes and liquid fractions. In fact, only the microgravity conditions obtained in space (for instance, inthe International Space Station) can be used to have foams at any liquid fractions remaining constant over long period of times.

2.8. Film Rupture. Another general mechanism by which foams evolve is the coalescence of neighboring bubbles via film rupture. This occurs if the nature of the surface-active components is such that the repulsive interactions and Marangoni flows are not sufficient to keep neighboring bubbles apart. Bubble coalescence can become more frequent as the foam drains and there is less liquid to separate neighbors. Long-lived foams can be easily formulated in which film rupture is essentially negligible, by ensuring that the surface-active agents provide a sufficiently large barrier that prevents the two films from approaching each other. Then film rupture is probably a thermally activated process in which a large, rare fluctuation away from equilibrium thickness and over an energy barrier is needed. Film rupture can also be enhanced by mechanical shock. Other external perturbations such as thermal cycling, mechanical shearing, composition change via evaporation or chemical or particulate additives, can also greatly affect the rate of film rupture (see DEFOAMERS).

2.9. Gas Diffusion. For very long-lived foams, film rupture is negligible and drainage slows to a stop as hydrostatic equilibrium is attained. Nevertheless, the foam is still not in thermodynamic equilibrium and continues to evolve with time. This occurs through an entirely different, though very general, means:gas diffusion. Smaller bubbles have a greater interfacial curvature and hence, by Laplace's law, have a higher internal pressure than larger bubbles. This results in a diffusive flux of gas from smaller to larger bubbles. Thus with time small bubbles shrink while large bubbles grow. This process is known as coarsening, or ripening, and results in the net increase in the average bubble size over time. It is ultimately driven by surface tension and serves to decrease the total interfacial surface area with time. This process has many similarities to the phase separation of binary liquids and metal alloys (45–47).

As coarsening proceeds, the distribution of bubbles changes so that the average bubble size gets larger with time. The evolution of the bubble size distribution is typically expected to be self-similar; ie, the distribution is independent of time when scaled by the average bubble size which, in turn, grows as a power of time (45,46) Any means of characterizing foam structure can be used to study foam evolution provided that the measurement can be made noninvasively and sufficiently rapidly. Thus the measurement techniques that require the foam to be destroyed, such as cryomicroscopy, are not really suitable to study the stability of the foam. One technique that has been applied successfully is the measurement of the change in the pressure head over an evolving foam. This can be related to the total change in interfacial surface area (48,49), and provides a measure of evolution, and hence stability of the foam. Also, multiple light scattering techniques (in both static and dynamic modes) have been used to follow the time

evolution of a foam (24,50). With these techniques, evidence of scaling regimes have been found and the exponent of the bubble size growth law measured close to ½, as expected when the cells are packed and deformed (45).

The overall rate constant, as opposed to the growth exponent, depends directly on such material parameters as the surface tension, the solubility and diffusion constant of gas molecules in the interstitial liquid, the film thickness and the liquid content (40,41). Note that the dependence with the liquid fraction is not yet completely known (as measuring the coarsening of wet foams, at constant liquid fraction, is very difficult because of drainage). The studies of sound propagation into foams also turned out to be an indirect method to measure the coarsening (51).

During coarsening, some bubbles shrink and others grow, and it is interesting to determine for a given bubble what sets the sign of its growth rate. For two-dimensional (2D) foams, it is known that only the number of edges n of a bubble is crucial : bubbles with $n<6$ shrink while those with $n>6$ grow (von Neumann's law). A statistical version of the von Neumann law for 3D dry foams has long been conjectured (with the number of faces replacing the number of edges), with both theoretical and experimental work. (18,52). Recently an analytical version of such a law has been derived by Hilgenfeldt and co-workers (53), which is in good agreement with measurements and simlations. From all these studies, it turns out that bubble having 13 faces or less shrink, while bubble with more faces grow.

Coarsening not only alters the size distribution, but alters the foam topology as well (12). Local stresses arise due to the change in packing conditions as small bubbles shrink and large bubbles grow. These stresses can be relieved by topology changes in which a bubble's nearest neighbors are changed (24). These discrete rearrangements also exhibit temporal scaling (50).

A common engineering technique for determining foam stability entails measuring the amount of foam produced. For defoaming applications, this is often a more important measure of stability than the foam structure.

2.10. Rheology. The rheology of foam is striking; it simultaneously shares the hallmark rheological properties of solids, liquids, and gases. Like an ordinary solid, foams have a finite shear modulus and respond elastically to a small shear stress. However, if the applied stress is increased beyond the yield stress, the foam flows like a viscous liquid. In addition, because they contain a large volume fraction of gas, foams are quite compressible, like gases. Thus foams defy classification as solid, liquid, or vapor, and their mechanical response to external forces can be very complex. Note also that, at rest, foams are athermal systems because the thermal energy is much smaller than the typical barrier for bubbles to change their relative positions. This results in a jammed configuration of the bubbles.

One simple rheological model that is often used to describe the behavior of foams is that of a Bingham plastic. This applies for flows over length scales sufficiently large that the foam can be reasonably considered as a continuous medium. The Bingham plastic model combines the properties of a yield stress like that of a solid with the viscous flow of a liquid. In simple Newtonian fluids, the shear stress τ is proportional to the strain rate γ, with the constant of proportionality being the fluid viscosity. In Bingham plastics, by contrast, the relation

between stress and strain rate is $\tau = \tau_y + \mu_p \dot{\gamma}$, where τ_y is the yield stress below which there is no flow and μ_p is called the plastic viscosity. The effective viscosity is thus given by $\mu = \mu_p + \tau_y/\dot{\gamma}$ and is therefore shear thinning.

Consistent with this model, foams exhibit plug flow when forced through a channel or pipe. In the center of the channel the foam flows as a solid plug, with a constant velocity. All the shear flow occurs near the walls, where the yield stress has been exceeded and the foam behaves like a viscous liquid. At the wall, foams can exhibit wall slip such that bubbles adjacent to the wall have nonzero velocity. The amount of wall slip present has a significant influence on the overall flow rate obtained for a given pressure gradient.

While the Bingham plastic model is an adequate approximate description of foam rheology, it is by no means exact. More detailed models attempt to relate the rheological properties of foams to the structure and behavior of the bubbles.

For very dry foams, the rheological properties are determined solely by the films separating the bubbles. The rheological properties of a set of randomly oriented films were determined first by Derjaguin (54) and later independently by Stamenovic and Wilson (55). These models set the scale for the elastic modulii of a foam. In the dry limit (when the gas fraction equals 1), the bulk modulus of the foam is dominated by that of the gas in the bubbles, whereas the shear modulus is given by $G0.55\sigma/R$, where σ and R are the surface tension and mean bubble radius. The bulk modulus of an ideal gas is equal to its pressure, so that for typical foams, the shear modulus is considerably weaker than the bulk modulus.

The model of randomly oriented thin films was made more precise through detailed micromechanical models that considered a 2D array of hexagonal bubbles of equal sizes (56). Again only the surface tension of the thin films was considered. Because of the simpler geometry, the model could be solved exactly in two dimensions. Nevertheless, it provides considerable insight. It establishes the physical basis for the elastic modulus, which is the stretching of films with a shear deformation, as shown in Figure 4. The increased surface area results in a restoring force, providing the elastic model. It also suggests an origin for the yield stress; when the foam is sheared enough that the bubbles can slide over one another, the foam yields. This micromechanical model has been further refined through computer simulations, mainly restricted to two dimensions (57–60). This type of computer modeling has been extended to ordered 3D structures (61). Simulations in 2D foam remain today quite useful, as they already catch many features of the 3D behavior, while being much more simple to perform. The linear rheology for various liquid fractions, as well as the nonlinear flow regimes, have recently been studied (62).

Studies with 2D foams have the advantage that all the bubbles are always seen, as well as their degree of deformation. In that sense, methods based on the direct observation and measurement of a statistical strain inside the foam have been developped, with the introduction of a statistical texture tensor which allow to quantify the notion of stored deformation. Such approaches extend the definition of the elastic strain for systems with both elastic and fluid properties (63).

The linear rheology of foams can be studied by rheological oscillation experiments, from which the elastic (or storage) modulus G' and the visocus (loss)

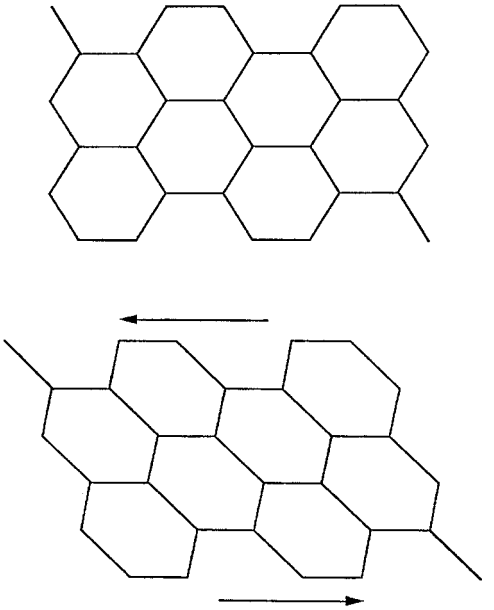

Fig. 4. Schematic representation of a 2D model to account for the shear modulus of a foam. The foam structure is modeled as a collection of thin films; the Plateau borders and any other fluid between the bubbles is ignored. Furthermore, all the bubbles are taken to be uniform in size and shape. When shear is applied, the total area of the thin films increases, and the surface tension results in a restoring force, providing the shear modulus of the foam.

modulus G'' are measured. In a large range of frequencies, these moduli are almost constant, with $G'/G'' \sim 10$ for dry foams with liquid fraction of a few percent (64). At high frequencies, anomalous viscous loss have been observed, both in foams and emulsions, and related to the occurrence of weak planes, randomly oriented, where layers of bubbles slip relatively to each other (65). The response at low frequency is much more difficult to study as experiments require long measurement times, so that the foam may evolve widely both by drainage and coarsening. In fact, the coarsening process is crucial as it induces local bubble rearrangements, and the cumulative effects of many coarsening-induced rearrangements is able to relax at long times (thus corresponding to the low frequency range) a macroscopically imposed stress. As a result, at low frequencies, the loss modulus G'' becomes much bigger than G', and is proportional to the frequency, as for an ordinary equilibrium liquid (66).

The shear modulus of wet foams must ultimately go to zero as the volume fraction of the bubbles decreases. The foam only attains a solid-like behavior when the bubbles are packed at a sufficiently large volume fraction that they begin to deform. In fact, it is the additional energy of the bubbles caused by their deformation that must lead to the development of a shear modulus. Experiments show that the dependence of the elastic modulus with the liquid fraction follows an universal behavior (64), also found and discussed for emulsions (67),

once the moduli are normalized by the Laplace pressure σ/R. Apart the change of surface tension, changing the surfactants and the physical chemistry of the bubble interfaces and thin films do not change the elastic response of the foam: No microscopic parameters linked to the surface viscoelasticity need to be taken into account. In foams the surface tension remains always so high (a few tens of mM/m) that it hides the other possible origins of elasticity. However, this is not the case for the G'', which is much more dependent on the physical chemistry of the foam. The microscopic mechanisms for the dissipation at the surfaces and in the films, in the linear rheology regim, are not yet well understood, and could come from various dissipative processes (68).

The viscous behavior of the foam once it begins to flow has also been investigated, both theoretically (69–71) and experimentally (72). The use of complementary techniques, associated with macroscopic rheology, like the diffusing wave spectroscopy (DWS) provided a means to determine the relations between the dynamic processes at the scale of a bubble and the macroscopic properties (73). Applying a shear to foam is indeed another way to unjam its bubbles, and to induce a continuous flow. The higher the shear rate, the lower the viscosity, and the more liquid-like the foam behave. At the scale of the bubbles, it is shown that at low shear rates the foam flow by discrete localized intermittent rearrangements. As the shear rate is increased, there is a cross-over to a regime where the bubble motion becomes smooth and uniform, completely controlled by the applied shear. The interesting critical strain rate associated to this cross-over is equal to the yield strain (typically a few percent) divided by the duration of a single local rearrangement (0.1s). It has also been possible to study the dynamics of rejamming (or $\gg$ solidification), after an applied shear has unjammed (melted) the foam (74). It is then shown that here again the coupling between coarsening and rheology is important.

It is thus possible to unjam a foam (induce a jamming transition) via different ways: First by simply increasing the liquid content so that the bubbles are less and less packed, second, by applying a shear rate which induce bubble motions, and lastly with time as the coarsening process, relaxing all the stresses and also creating bubble rearrangements. The concepts discussed here about jammed systems and jamming transition are in fact valid for a whole class of materials, including foams, and sharing the same basic ingredients (disorder and yielding). Pastes, emulsions, glasses, granular materials and suspensions are other materials of this family. A generic jamming phase diagram has been proposed by Liu and co-workers, with three axis (temperature, inverse of the packing fraction, and applied shear stress) (75,76). Close to the origin a system is jammed, and it crosses a jamming transition as it is moved away from this origin on any possible path. Another general issue for this kind of athermal systems, once driven by shear, is to know if they could possibly be described within the statisitical physics framework but with an effective temperature (depending on the shear rate). In that spirit, phenomenological approaches have been used with some sucess (77), and recent simulations have shown that the concept of effective temperature should be useful for any systems near the onset of jamming (78).

2.11. Measurement. To determine rheological parameters such as the yield stress and effective viscosity of a foam, commercial rheometers are available

(79); rotational (couette cell or cone-plate geometry, eg,) and continuous-flow-tube viscometry are most commonly employed (see RHEOLOGICAL MEASUREMENTS). However, obtaining reproducible results independent of the sample geometry is nevertheless a difficult goal. First, because foams always evolve by drainage and coarsening and that all these effects are coupled, inducing changes of the rheological behavior. Also because of possible nonuniform shear conditions due either to wall slip, or to shear localization effects (shear banding). For example, viscous dissipation in wall slip depends sensitively on the thickness of wetting layer of liquid that intrudes between the wall and the foam bubbles; this layer thickness varies greatly with surface chemistry and liquid composition and can also change with time as the foam drains. All these possible non-uniform deformation effects still need to be investigated in details, as well as their effective role in the macroscopic rheological measurements. More complex rheological phenomena are also expected in foams like dilatancy effects (31) or non-zero normal stress differences.

3. Production

Several techniques are available for the generation of special-purpose foam with the desired properties. The simplest method is to disperse compressed gas directly into an aqueous surfactant solution by means of a glass frit. A variation of this method that allows for control of liquid content is to simultaneously pump gas and surfactant solution through a bead pack or steel wool, for example, at fixed rates. In the same spirit, another solution, which can be used for laboratory purposes, consists of pushing a pressurized surfactant solution through a single pinhole, and to add any desired gas flow rate just after that pinhole. Large amount of foams, at any liquid fractions, are then produced by the subsequent turbulent mixing of these fluids inside a final tube of confinement (80). Less reproducible mechanical means of foam generation include brute force shaking and blending. For highly reproducible foams composed of small bubbles, such as shaving creams, the aerosol technique is especially suitable (81) (see AEROSOLS). Hydrocarbons or chlorofluorocarbons are liquefied at high pressure and then emulsified with the surfactant solution. When released to atmospheric pressure, the propellant droplets evaporate into tiny gas bubbles which aggregate into a foam.

4. Applications

Foams have a wide variety of applications that exploit their different physical properties. The low density, or high volume fraction of gas, enable foams to float on top of other fluids and to fill large volumes with relatively little fluid material. These features are of particular importance in their use for fire fighting. The very high internal surface area of foams makes them useful in many separation processes. The unique rheology of foams also results in a wide variety of uses, as a foam can behave as a solid, while still being able to flow once its yield stress is exceeded.

Foams are also widely encountered in circumstances where their presence is detrimental. Foams are common to many processes that entail agitation of fluids or bubbling of air through fluids. The presence of any type of surface-active ingredient, even in minute quantities, enhances the formation of foams in the processing. The presence of the foams increases the volume of the fluids and makes them more difficult to process and transport. Moreover, foams can have strong detrimental environmental effects. Thus, just as the production and stabilization of foams is important in some industrial processes, so the elimination of foams is crucial in many others. As a result, a wide variety of defoaming agents have been developed to eliminate or reduce the formation of foams (see DEFOAMERS).

4.1. Firefighting. Foams are widely used in firefighting applications (82). They are particularly useful in extinguishing flammable liquids, eg, gasoline. Whereas water simply agitates the gasoline, further spreading the fire, and then sinks to the bottom of the burning fluid, a foam is less dense than the burning liquid, and remains suspended on its surface. The collapsing bubbles cool the fluid near the surface, and reduce the amount of oxygen available to the flame, ultimately extinguishing it. A foam is also a more efficient use of the firefighting liquid, typically water, enabling it to be spread over a much larger area.

Foams for firefighting applications are typically made from a concentrated foaming agent diluted with water and then mixed with air. Rather than consider the volume fraction of air in the foam, firefighting foams are characterized by their expansion ratio, which is the increase in volume of the liquid after the foam is formed. Expansion ratios range from 5:1 to >1000:1; ratios of 5:1–20:1 are called low expansion; ratios of 21:1–200:1, medium expansion; and ratios >200:1, high expansion.

Low expansion foams are used most commonly. Because they are relatively more dense, they can more easily be sprayed larger distances, making them safer to use. In addition, because of the larger amount of liquid, they are more resistant to the heat of the fires, making them more effective as extinguishers. Their primary disadvantage is the relatively smaller area that they can cover due to their lower expansion ratio. Medium expansion foams are usually too light to be sprayed any distance, and instead must be formed very near to the flames. However, they can cover a much larger area of flame, and the low density reduces the probability of disrupting the surface of the burning fluid. They are less heat resistant and hence more easily destroyed than low expansion foams. However, they can cover a much greater area. High expansion foams cover the widest area, but suffer from even poorer heat resistance, and virtually no ability to be sprayed. Hence they are typically formed in place, and are often used to fill the places where a fire has already started, such as in the holds of ships, warehouses, or mines. They are also sometimes used in fighting forest fires in areas where water is scarce.

Most foam-forming concentrates used contain some form of protein, usually derived from animals. In addition, many contain fluorochemical surfactants to increase their foaming performance. Other foaming agents are comprised solely of synthetic surfactants. Most foams produced with either protein-based or synthetic foaming agents are susceptible to polar fluids, particularly alcohols, which are miscible in water and tend to destroy the firefighting foams. As a result,

all-purpose foaming agents have been developed that produce foams which are not destroyed by alcohols, and are effective in fighting all types of fires. They typically contain natural polymers that are insoluble in polar solvents.

4.2. Food. Foams are common to a wide variety of food products. Whipped cream and meringue are essentially foams, and ice cream is comprised of a large amount of foam. These foams are stabilized by proteins; the two most important are egg white and milk proteins. For food products, it is desirable not only to achieve good foaming properties, but also to form stable foams (83–86). The ease with which foams are formed depends on the capacity of the proteins to rapidly adsorb onto the interface. The stability of the foams depends on the ability of the proteins to form an elastic membrane at the interface, which both prevents bubble coalescence and is sufficiently impermeable to reduce gas diffusion. One of the best food-foaming agents is egg white or egg albumen. It consists of a mixture of different proteins, each serving a particular function (87). Globulins are the most surface-active agents, leading to good foamability; drainage is retarded by the high viscosity caused by globulins and ovomucoids; the film strength is enhanced by surface complexes formed between lysozymes and ovomucins. Upon heating, thermal denaturation of ovalbumin and conalbumin results in a more permanent foam structure, leading to its widespread use in baked products. Ice cream is also a type of foam possessing varying amounts of air bubbles incorporated during an aeration step in the processing (88). These bubbles are initially stabilized by milk proteins, primarily β-casein, α-lactalbumin, and β-lactoglobulin (89). Further stabilization occurs due to the adsorption of fat globules on the interface.

Another important digestible foam is that on the top of a glass of freshly poured beer (qv). Although not as long lasting, it is nevertheless considered an important aesthetic quality of the beverage, and is thus the subject of considerable research (90,91). In addition, its aesthetic importance is somewhat dependent on location. For example, beer in the United Kingdom has traditionally possessed a higher and longer lasting head of foam than that in the United States. The foam in beer is usually formed by the dissolved CO_2, although dissolved nitrogen has also been used to improve the quality. The main stabilizer in the foam is proteins in the beer, although other components, such as trace metal ions, iso-α-acids, and propylene glycol alginate (PGA), also enhance the stability of beer foam. In fact, PGA is also sometimes added to beer to improve the foam (92).

4.3. Separations. Foams have important uses in separations, both physical and chemical (93,94). These processes take advantage of several different properties of foams. The buoyancy and mechanical rigidity of foam is exploited to physically separate some materials. The large volume of vapor in a foam can be exploited to filter gases. The large surface area of a foam can also be exploited in the separation of chemicals with different surface activities.

Froth flotation (qv) is a significant use of foam for physical separations. It is used to separate the more precious minerals from the waste rock extracted from mines. This method relies on the different wetting properties typical for the different extracts. Usually, the waste rock is preferentially wet by water, whereas the more valuable minerals are typically hydrophobic. Thus the mixture of the two powders are immersed in water containing foam promoters. Also added

are modifiers which help ensure that the surface of the waste rock is hydrophilic. Upon formation of a foam by bubbling air and by agitation, the waste rock remains in the water while the minerals go to the surface of the bubbles, and are entrapped in the foam. The foam rises, bringing the minerals to the surface with it. This can be collected, and the valuable minerals, now higher in purity, extracted.

Foam fractionation is a separation method that is chemical in origin (94). It relies on the preferential surface adsorption of some molecules and hence exploits the large surface area of foams. This is a commonly used method for separating surfactant molecules. It can be extended to other separations by coating the material to be separated by surfactant to enhance its adsorption at the surface. For example, foam fractionation has been applied to remove radioactive wastes. An advantage of this method is that the foam can be spread over a large contaminated volume, but the actual amount of material containing the radioactive waste is quite small, once the foam has been drained and collapsed. Foams can also be used to collect and separate small colloidal particles, if they are coated with a surfactant to bring them to the interface. Another use of foams are in the deinking processing to recycle waste paper. Air bubbles are used to remove the ink from the paper, and these are collected and separated as a foam.

4.4. Oil Recovery. Foams find wide use in oil recovery, from the initial drilling of the bore holes, through the first recovery stage, and, increasingly, all the way to tertiary or enhanced oil recovery. Again, this application exploits the unique features of foams, primarily the large interfacial area and the distinctive rheological properties of flowing foams.

In the drilling of oil wells, foam is sometimes used as the drilling fluid. Usually the drilling fluid is a clay or mud slurry, which is circulated down the bore hole to remove the waste generated by the drilling process, and to seal the well, preventing the expulsion of oil that is under pressure. However, in some wells, the pressure of the oil in the ground is less than the pressure head generated by a water column the height of the well. Thus a drilling mud would exert excessive pressure, and could contaminate the rock structure near the bore hole. In these cases, an aqueous foam is often used. It has all the features of a drilling mud, and can also aid in cleaning the drilling material from the well. However, since its density is lower, the pressure exerted by the drilling fluid on the oil is reduced.

Foams are also used in extracting the oil from the ground. One important use is in controlling the flow of fluids in the rock formation. The most common form of secondary oil recovery entails pushing the oil out of the ground by flooding the formation with water from one well and collecting the oil that is pushed out from an adjacent well. This process suffers from several problems that may be alleviated with foams. One problem is encountered if the rock formation contains channels of higher permeability, or lower resistance to the flow of fluids. These may arise, eg, from fractures in the formation. The water being forced through the formation flows more easily through these high permeability channels, bypassing the rest of the formation and greatly reducing the effectiveness of the recovery, or the sweep efficiency. One method that is sometimes used to alleviate this problem is the injection of foam-forming materials into the formations. The foam tends to go first into these larger channels, and then plugs them.

By contrast, in the narrower channels, the shear stresses on the foam are larger, causing it to flow. This effectively blocks the high permeability regions and forces the pushing fluid to flow in the remainder of the formation, making it more effective in removing the oil. Another almost opposing use of foam is as a pressurizing agent to fracture the formation. This technique is used for very viscous oils, such as tar sands. These fractures then provide channels to allow the penetration of hot steam which is used to lower the viscosity of the heavy oil to enhance its flow. Sand is often added to fill the cracks and prop them open. When a foam is used as the pressurizing fluid, the settling of the sand during the injection is minimized (95).

Foam is also increasingly being considered in tertiary oil applications. Even with the water floods used in secondary oil recovery, typically 30–60% of the oil remains in the ground. Enhanced oil recovery, or tertiary recovery techniques, are used to try to extract this remaining oil. This is generally done by decreasing the interfacial tension of the oil, which is accomplished either through the use of a surfactant, or through the use of a miscible flood, where the pushing fluid is miscible in the oil. One type of miscible flooding uses the injection of CO_2, or other gases, which form a foam that displaces the oil (96). Foams also help control the mobility of the pusher. Often the oil that is being displaced has a higher viscosity, and thus a lower mobility, than the displacing fluid. Then the flow can become unstable, and instead of a uniform front of the displacing fluid advancing through the formation, narrow fingers are formed (97). This viscous fingering instability can greatly reduce the sweep efficiency. The occurrence of this instability can be reduced by decreasing the mobility of the pushing fluid. The use of foams are one technique for achieving this. This use exploits the rheological properties of the foams. More generally, the flow of foams in the very narrow pore spaces of an oil bearing formation is very complex, and is not completely understood (98). The behavior entails the motion of bubbles of air that can be comparable to the size of the pore spaces themselves. This can result in the bursting of the bubbles, which has the effect of introducing new interfaces into the flowing fluids. The flow of these interfaces, as well as the flow of the still intact bubbles themselves, in the restricted geometry of the pore spaces is a complex problem that is very sensitive to the nature of the rocks, the disorder of the pore spaces, and the local wetting properties of the formation. In addition, the flow of the interfaces, and the foam, at length scales larger than the pore space, but still smaller than the size of the whole oil field, remains a very poorly understood, and little investigated, problem. Thus, although foams have considerable promise for use in tertiary oil recovery, their applications have, to date, been limited.

4.5. Detergents. Foams are often associated with detergents, but they are generally not essential. Instead, foaminess is often a desirable trait more for its effect on the consumer than its function. In fact, excessive foaming can be detrimental to the cleaning if the volume of the foam is too high. One exception is the case where the cleansing action must be restricted to some particular region, and where excessive amounts of water must be avoided. For example, foams are often used to clean rugs, as they can spread the detergent on the surface of the rug, while avoiding excessively wetting the base of the rug.

4.6. Textiles. Foams are often encountered in the production of textiles (qv), which involves extensive interactions between the fibers, which have a large surface area, and a variety of aqueous treatments. In most cases, these foams

are detrimental to the processing and fabrication of the textiles and measures are taken to reduce the foaming (99). These include modifications of the mechanical fabrication techniques, addition of foam inhibitors, and the use of low foaming surfactants in the processing. However, in other instances, foams can be used advantageously in textile processing, primarily for the application of screen printing, coatings, backings, and certain types of dyes (100). Foams can also be used to clean textiles as the foam helps wet between the fibers thereby more effectively spreading the detergent.

4.7. Cosmetics. Besides the esthetic appeal of foams, they have two properties that are exploited for cosmetic purposes. The first is their ability to retain different substances and distribute them as required, while using a relatively small quantity of fluid. An example of this application is the lather formed by some shampoos, which effectively spreads the detergent by wetting the surfaces of the hair, while avoiding excessive liquid that would otherwise fall off. The second application is to spread a moisturizer or lubricant, while still providing enough resiliency to hold the fluid in place. A prime example of this is shaving cream, which provides both moisturization and lubrication for shaving.

4.8. Other. Because a foam consists of many small, trapped gas bubbles, it can be very effective as a thermal insulator. Usually solid foams are used for insulation purposes, but there are some instances where liquid foams also find uses for insulation (see FOAMED PLASTICS; INSULATION, THERMAL). For example, it is possible to apply and remove the insulation simply by forming or collapsing the foam, providing additional control of the insulation process. Another novel use that is being explored is the potential of absorbing much of the pressure produced by an explosion. The energy in the shock wave is first partially absorbed by breaking the bubbles into very small droplets, and then further absorbed as the droplets are evaporated (92).

Safety, Health, and Environment Foams play important roles in environmental issues, both beneficial and detrimental.

4.9. Natural Waters. Many water systems have a natural tendency to produce foam upon agitation. The presence of pollutants exacerbates this problem. This was particularly severe when detergents contained surfactants that were resistant to biodegradation. Then, water near industrial sites or sewage disposal plants could be covered with a blanket of stable, standing foam (94,101). However, surfactant use has switched to biodegradable molecules, which has greatly reduced the incidence of these problems.

4.10. Wastewater Treatment. The treatment of wastewater, either from sewage or from industrial processes, typically entails a preliminary filtration to remove the large volumes of solids, and then a slower settling to remove the sand and gravel (see WATER, SOURCES AND QUALITY ISSUES). The water is then treated by an activated sludge process to remove the remaining dissolved solids and organic colloidal particles. Activated sludge is a biomass that assists in the degradation of the organic waste in the water. The process entails a mixing and aeration of the wastewater with the activated sludge, which can lead to problems of foaming. The foams produced can be quite stable, resulting in additional problems for waste disposal. The foams produced in this process differ from those normally encountered in that the foam producing and stabilizing agents are microbial, primarily including Nocardia (102,103), Microthrix parvicella

(104,105), and Rhodococcus (106,107). These foams are more difficult to treat with defoaming agents. Moreover, it is very difficult to predict the degree of foamability of the waste being treated (108). In other, more specialized wastewater treatments, these problems do not arise, and defoaming agents can be used effectively. For example, the wastewater remaining from the pulp used in the production of paper (qv) contains dissolved soaps from fatty acids and abietes, which can lead to foam problems. These can be controlled with mixtures of organic solvents and nonionic surfactants (109) or with gaseous sulfur dioxide (99).

4.11. Chlorofluorocarbon Alternatives. There still is no completely satisfactory propellant for use in the aerosol method of foam production (81). Chlorofluorocarbons, still widely used, are harmful to atmospheric ozone and low molecular weight hydrocarbons, now popular, eg, in producing shaving cream, are explosive and promote the greenhouse effect. The difficulty is in creating a safe, stable liquid that can be readily emulsified and whose vapor pressure at room temperature is roughly 200–300 kPa (2–3 atm).

BIBLIOGRAPHY

"Foams" in *ECT* 1st ed., Vol. 6, pp. 772–778 by E. I. Valko, Polytechnic Institute of Brooklyn; in *ECT* 2nd ed., Vol. 9, pp. 884–901 by L. Shedlovsky, Colgate-Palmolive Co.; in *ECT* 3rd ed., Vol. 11, pp. 127–145 by S. Ross, Rensselaer Polytechnic Institute; in *ECT* 4th ed., Vol. 11, pp. 783–805 by Douglas J. Durian, UCLA and David A. Weitz, Exxon Research & Engineering Company; "Foams" in *ECT* (online), posting date: December 4, 2000 by Douglas J. Durian, UCLA and David A. Weitz, Exxon Research & Engineering Company.

CITED PUBLICATIONS

1. M. J. Rosen, *Surfactants and Interfacial Phenomena*, John Wiley & Sons, Inc., New York, 1989.
2. M. Dahanayake, A. W. Cohen, and M. J. Rosen, *J. Phy. Chem.* **90**, 2413 (1986).
3. P. Lianos and R. Zana, *J. Colloid Interface Sci.* **84**, 100 (1981).
4. J. N. Israelachvili, *Intermolecular and Surface Forces*, Academic Press Ltd., San Diego, 1991.
5. B. V. Derjaguin and L. Landau, *Acta Physicochim. USSR* **14**, 633 (1941).
6. E. J. W. Vervey and J. T. G. Overbeek, *Theory of the Stability of Lyophobic Colloids*, Elsevier, Amsterdam, 1948.
7. J. S. Clunie, J. F. Goodman, and P. C. Symons, *Nature (London)* **216**, 1203 (1967).
8. V. Bergeron *J Phys: Condens Matter* **11**, R215 (1999).
9. C. Stubenrauch, and R. v. Klitzing, *J. Phys.: Condens. Matter* **15**, R1197 (2003).
10. D. Weaire and R. Phelan, *Nature (London)* **367**, 123 (1994).
11. E. B. Matzke, *Am. J. Bot.* **33**, 58 (1946).
12. D. Weaire and N. Rivier, *Contemp. Phys.* **25**, 55 (1984).
13. C. Isenberg, *The Science of Soap Films and Soap Bubbles*, Dover Publications, New York, 1992.
14. J. E. Avron and D. Levine, *Phys. Rev. Lett.* **69**, 208 (1992).
15. H. C. Cheng and R. Lemich, *Ind. Eng. Chem. Fundam.* **22**, 105 (1983).

16. A. Selecki and R. Wasiak, *J. Coll. Interface Sci.* **102**, 557 (1984).
17. C. Monnereau, and M. Vignes-Adler, *Phys. Rev. Lett.* **80**, 5228 (1998).
18. A. J. Wilson, ed., *Foams: Physics, Chemistry, and Structure*, Springer-Verlag, New York, 1989, p. 69.
19. The "Surface Evolver" sofware is available free at: http://www.susqu.edu/facstaff/b/brakke/evolver
20. A. Kraynik, D. Reinelt, and F. van Swol, *Phys. Rev. E* **67**, 031403 (2003).
21. N. O. Clark, *Trans. Faraday Soc.* **44**, 13 (1948).
22. A. K. Agnihotri and R. Lemlich, *J. Colloid Interface Sci.* **84**, 42 (1981).
23. R. Phelan, D. Weaire, E. A. J. F. Peters, and G. Verbist, *J. Phys. Condens. Matter* **8**, L475 (1996).
24. D. J. Durian, D. A. Weitz, and D. J. Pine, *Science* **252**, 686 (1991).
25. M. U. Vera, A. Saint-Jalmes, and D. J. Durian, *Appl. Opt.* **40**, 4210 (2001).
26. A. S. Gittings, R. Bandyopadhyay, and D. J. Durian, *Europhys. Lett.* **65**, 414 (2004)
27. S. J. Cox, D. Weaire, S. Hutzler, J. Murphy, R. Phelan, and G. Verbist, *Proc. R. Soc. London A* **456**, 2441 (2000).
28. A. Saint-Jalmes, M. U. Vera, and D. J. Durian, *Europhys. Lett.* **50**, 695 (2000).
29. A. Saint-Jalmes and D. Langevin, *J. Phys.: Condens. Matter* **14**, 9397 (2002).
30. S. A. Koehler, S. Hilgenfeldt, and H. A. Stone, *Langmuir* **16**, 6327 (2000).
31. D. Weaire, S. Hutzler, S. Cox, N. Kern, M. A. Alonso, and W. Drenckhan, *J. Phys.: Condens. Matter* **15**, S65 (2003).
32. H. A. Stone, S. A. Koehler, S. Hilgenfeldt, and M. Durand, *J; Phys. Condens. Matter* **15**, S283 (2003).
33. R. A. Leonard and R. Lemlich, *AIChE J.* **11**, 18 (1965).
34. A. Saint-Jalmes, Y. Zhang, D. Langevin, to appear in *Eur. Phys. J. E* (2004).
35. S. A. Koehler, S. Hilgenfeldt, E. R. Weeks, and H. A. Stone, *J. Coll. Interface Sci.*, *in press*.
36. S. A. Koehler, S. Hilgenfeldt and H. A. Stone, *J. Coll. Interface Sci.*, *in press*.
37. K. J. Mysels, K. Shinoda, and S. Frankel, *Soap Films, Studies of Their Thinning and a Bibliography*, Pergamon Press, New York, 1959.
38. J. Lyklema, P. C. Scholten, and K. J. Mysels, *J. Phys. Chem.* **69**, 116 (1965).
39. I. B. Ivanov, *Thin Liquid Films: Fundamentals and Applications*, Marcel Dekker, Inc., New York, 1988.
40. S. Hilgenfeldt, S. A. Koehler, and H. A. Stone, *Phys. Rev. Lett.* **86**, 4704 (2001).
41. M. U. Vera and D. J. Durian, *Phys. Rev. Lett.* **88**, 088304 (2002).
42. H. M. Princen, *J. Coll. Interface Sci.* **134**, 188 (1989).
43. S. Hutzler, D. Weaire, and R. Crawford *Europhys. Lett.* **41** 461 (1998).
44. M. U. Vera, A. Saint-Jalmes, and D. J. Durian, *Phys. Rev. Lett.* **84**, 3001 (2001).
45. A. J. Markworth, *J. Coll. Interface Sci.* **107**, 569 (1984).
46. W. W. Mullins, *J. Appl. Phys.* **59**, 1341 (1986).
47. J. A. Glazier, S. P. Gross, and J. Stavans, *Phys. Rev. A* **36**, 306 (1987).
48. G. Nishioka and S. Ross, *J. Coll. Interface Sci.* **81**, 1 (1981).
49. A. Monsalve and R. S. Schechter, *J. Coll. Interface Sci.* **97**, 327 (1984).
50. D. J. Durian, D. A. Weitz, and D. J. Pine, *Phys. Rev. A* **44**, R7902 (1991).
51. N. Mujica and S. Fauve, *Phys. Rev. E* **66**, 021404 (2002).
52. J. A. Glazier, *Phys. Rev. Lett.* **70**, 2170 (1993).
53. S. Hilgenfeldt, S. A. Koehler, and H. A. Stone, *Phys. Rev. Lett.* **86**, 2685 (2001).
54. B. V. Derjaguin, *Kolloid-Zeitschrift* **64**, 1 (1933).
55. D. Stamenovic and T. A. Wilson, *J. Appl. Mechan.* **51**, 229 (1984). D. Stamenovic, *J. Coll. Interface Sci.* **145**, 255 (1991).
56. H. M. Princen, *J. Coll. Interface Sci.* **91**, 160 (1983).

57. F. Bolton and D. Weaire, *Phys. Rev. Lett.* **65**, 3449 (1990).
58. T. Herdtle and H. Aref, *J. Fluid Mech.* **241** 233 (1992).
59. T. Okuzono, K. Kawasaki, and T. Nagai, *J. Rheol.* **37**, 571 (1993).
60. D. A. Reinelt and A. M. Kraynick, *J. Fluid Mech.* **311**, 327 (1996).
61. D. A. Reinelt and A. M. Kraynick, *J. Coll. Interface Sci.* **159**, 460 (1993).
62. D. J. Durian, *Phys. Rev. E* **55**, 1739 (1997).
63. M. Aubouy, Y. Jiang, J. A. Glazier, and F. Graner, *Granular Matter* **5**, 64 (2003). M. Asipauskas, M. Aubouy, J. A. Glazier, F. Graner, and Y. Jiang, *Granular Matter* **5**, 71 (2003).
64. A. Saint-Jalmes and D. J. Durian, *J. Rheol.* **43**, 1411 (1999).
65. A. J. Liu; S. Ramaswami, T. G. Mason, H. Gang, and D. Weitz, *Phys. Rev. Lett.* **76**, 3017 (1996).
66. A. D. Gopal and D. J. Durian, *Phys. Rev. Lett.* **91**, 188303 (2003).
67. T. G. Mason M. D. Lacasse, G. S. Grest, D. Levine, J. Bibette, and D. A. Weitz, *Phys. Rev. E* **56**, 3150 (1997).
68. D. M. A. Buzza, C.-Y. D. Lu, and M. E. Cates, *J. Phys. II France* **5**, 37 (1995).
69. S. A. Khan and R. C. Armstrong, J. Non-Newtonian *Fluid Mech.* **25**, 61 (1987).
70. A. M. Kraynik and M. G. Hansen, *J. Rheol.* **31**, 175 (1987).
71. L. W. Schwartz and H. M. Princen, *J. Coll. Interface Sci.* **118**, 201 (1987).
72. H. M. Princen and A. D. Kiss, *J. Coll. Interface Sci.* **128**, 176 (1989).
73. A. D. Gopal and D. J. Durian, *J. Coll. Int. Sci.* **213**, 169 (1999).
74. S. Cohen-addad and R. Hohler, *Phys. Rev. Lett.* **86**, 4700 (2001).
75. A. J. Liu, and S. R. Nagel, *Nature (London)* **396**, 21 (1998).
76. A. J. Liu and S. R. Nagel, eds., *Jamming and Rheology*, Taylor and Francis, New York (2001).
77. P. Sollich, F. Lequeux, P. Hebraud, and M. Cates, *Phys. Rev. Lett.* **78**, 2020 (1997).
78. I. Ono, C. Ohern, D. J. Durian, S. Langer, A. Liu, and S. Nagel, *Phys. Rev. Lett.* **89**, 095703-1 (2002).
79. J. P. Heller and M. S. Kuntamukkula, *Ind. Eng. Chem. Res.* **26**, 318 (1987).
80. A. Saint-Jalmes, M. U. Vera, D. J. Durian, *Eur. Phys. J. B* **12**, 67 (1999).
81. P. A. Sanders, *Handbook of Aerosol Technology*, Van Nostrand Reinhold Co., New York, 1979.
82. F. Fitch, in Ref. , p. 207.
83. E. Dickinson, *Food Hydrocoll.* **1**, 3 (1986).
84. J. R. Mitchell, in B. J. F. Hudson, ed., *Developments in Food Proteins*, Elsevier Applied Science, London, 1986, p. 291.
85. S. Poole, and J. C. Fry, in B. J. F. Hudson, ed., *Developments in Food Proteins*, Elsevier Applied Science, London, 1987, p. 257.
86. A. Prins, in E. D. a. G. Stainsby, ed., *Advances in Food Emulsions and Foams*, Elsevier Applied Science, London, 1988, p. 91.
87. W. D. Powrie, in W. J. S. a. O. J. Cotterill, ed., *Egg Science and Technology*, Avi Publishing, Westport, Conn., 1977, p. 61.
88. J. K. Madden, in Ref. 14, p. 185.
89. M. Anderson, B. E. Brooker, and E. C. Needs, in E. Dickinson, ed., *Food Emulsions and Foams*, Royal Society of Chemistry, London, 1987, p. 100.
90. C. W. Bamforth, *J. Inst. Brewing* **91**, 370 (1985).
91. P. K. Hegarty, in Ref. 14, p. 197.
92. P. T. Slack, and C. W. Bamforth, *J. Inst. Brewing* **89**, 397 (1983).
93. R. Lemlich, *Adsorptive Bubble Separation Techniques*, Academic Press, Inc., New York, 1971.
94. J. J. Bikerman, *Foams*, Springer-Verlag, New York, 1973.

95. J. H. Aubert, A. M. Kraynik, and P. B. Rand, *Sci. Am.* **254**, 74 (1986).
96. F. I. Stalkup, Jr., *Miscible Displacement*, SPE, New York, 1983.
97. R. L. Chouke, C. van Meurs, and C. van der Pohl, *Pet. Tran. AIME* **216**, 188 (1959).
98. C. W. Nutt, and R. W. Burley, in Ref. , p. 105.
99. R. Hofer, and co-workers, in W. Gerhartz, ed., *Ullmann's Encyclopedia of Industrial Chemistry*, VCH, Weinheim, 1988, p. 465.
100. G. M. Bryant and H. T. Walter, *Handbook of Fiber Science and Technology*, Marcel Dekker, New York, 1983.
101. M. Raison, *Centre Belge Etude Doc. Eaux* **227**, 512 (1962).
102. H. Lemmer, *Korrespondenz Abwasser* **32**, 965 (1985).
103. O. J. Hao, P. E. Strom, and Y. C. Yu, *Water SA* **14**, 105 (1988).
104. J. R. Blackbeard, G. A. Ekama, and G. V. R. Marais, *Water Pollution Control* **85**, 90 (1986).
105. A. J. Goddard, and C. F. Forster, *Enzyme Microbial Tech.* **9**, 164 (1987).
106. M. Segerer, *Korrespondenz Abwasser* **31**, 1073 (1984).
107. T. Mori and co-workers, *Environ. Tech. Lett.* **9**, 1041 (1988).
108. C. F. Forster, in Ref. 14, p. 167.
109. K. Roberts, C. Axberg, and R. Osterlund, *Emulsion foam Killers Containing Fatty and Rosin Acids*, Brunel University, Uxbridge, U.K., 1975.

GENERAL REFERENCES

A. W. Adamson, *Physical Chemistry of Surfaces*, 4th ed., John Wiley & Sons, Inc., New York, 1982.
R. J. Akers, ed., *Foams: Proceedings of a Symposium Organized by the Society of Chemical Industry, Colloid and Surface Chemistry Group*, Brunel University, Uxbridge, U.K., Sept. 8–10, 1975, Academic Press, Inc., London, 1976.
G. R. Assar, and R. W. Burley, in N. P. Cheremisinoff, ed., *Encyclopedia of Fluid Mechanics*, Vol. 3, p. 26, Gulf Publishing Co., Houston, 1986, p. 26.
J. H. Aubert, A. M. Kraynik, and P. B. Rand, *Sci. Am.* **254**, 74 (May 1986).
J. J. Bikerman, *Foams*, Springer-Verlag, New York, 1973.
C. V. Boys, *Soap Bubbles: Their Colors and the Forces Which Mold Them*, Dover Publications, New York, 1959; originally published by the Society for Promoting Christian Knowledge, London, 1890.
H. C. Cheng, and T. E. Natan, in N. P. Cheremisinoff, ed., *Encyclopedia of Fluid Mechanics*, Vol. 3, Gulf Publishing Co., Houston, Tex., 1986, p. 3.
P. R. Garrett, *Defoaming: theory and Industrial Applications*, Surfactant Science series, New York, Marcel Dekker Inc., vol. 45 (1993).
J. P. Heller and M. S. Kuntamukkula, *Ind. Eng. Chem. Res.* **26**, 318 (1987).
C. Isenberg, *The Science of Soap Films and Soap Bubbles*, Dover Publications, New York, 1992; originally published by Tieto, Clevedon, U.K., 1978.
J. N. Israelachvili, *Intermolecular and Surface Forces, With Applications to Colloidal and Biological Systems*, Academic Press, Inc., San Diego, 1985.
A. M. Kraynik, *Ann. Rev. Fluid Mech.* **20**, 325 (1988).
K. J. Mysels, K. Shinoda, and S. Frankel, *Soap Films, Studies of Their Thinning and a Bibliography*, Pergamon Press, New York, 1959.
R. K. Prud'homme and S. A. Khan, *Foams, Theory, Measurements, and Applications*, Surfactant Science series, New York, Marcel Dekker Inc., Vol. 57, 1997.
M. J. Rosen, *Surfactants and Interfacial Phenomena*, 2nd ed., John Wiley & Sons, Inc., New York, 1989.

D. Weaire, and N. Rivier, *Contemp. Phys.* **25**, 55 (1984).
D. Weaire, and S. Hutzler, *The Physics of Foams*, Oxford University Press (1999).
A. J. Wilson, ed., *Foams: Physics, Chemistry and Structure*, Springer-Verlag, London, 1989.

ARNAUD SAINT-JALMES
Universite Paris-Sud
DOUGLAS J. DURIAN
University of Pennsylvania
DAVID A.WEITZ
Harvard University